A scale-aware dissipation mechanism for variable-resolution grids in CAM

Oksana Guba (SNL*), Michael Levy (NCAR), James Overfelt (SNL*), Mark Taylor (SNL*), Paul Ullrich (UC Davis)

SciDAC3 Project: Multiscale Methods for Accurate, Efficient, and Scale-Aware Models of the Earth System, PI: W. Collins

1. A coefficient dependent on scales

The traditional, well-tested hyperviscosity (HV) operator for uniform meshes is given by

$$\frac{\partial Q}{\partial t} = \nu \Delta^2 Q, \quad \nu = C(\Delta x_{unif})^s,$$

where Δx_{unif} is an *average* grid length and s is set to 3.2 or 4.0.

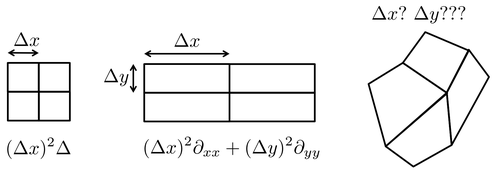

Figure 1: *Defining scales for hyperviscosity, non-uniform grids*

For the spectral element method, we compare two approaches for hyperviscosity on unstructured variable resolutioin grids:

1. **Scalar approach.** The simplest extension of the uniform mesh hyperviscosity. We use a spatially varying coefficient ν scaled based on the largest of the two length scales within each element. In regions of uniform resolution (low or high), this coefficient will match what is used on uniform grids. High resolutions use less dissipation, resolving finder scales. In transition regions, ν changes proportional to the element length scales.

$$\nu(x,y) = C \max(\Delta x, \Delta y)^s$$

$$\frac{\partial Q}{\partial t} = \nu(x,y)\, \Delta^2 Q \qquad (1)$$

2. **Tensor-based approach.** Use a tensor coefficient V. Within each spectral element, let D be the derivative of the map from the spectral element to the reference element (unit square). The eigenvectors of $D^T D$ give the coordinate system which diagonalizes the Laplace operator expressed in the reference element:

$$D^T D = E \begin{pmatrix} \lambda_1 & 0 \\ 0 & \lambda_2 \end{pmatrix} E^T$$

with eigenvalues $\lambda_1 \sim \Delta x^2$ and $\lambda_2 \sim \Delta y^2$. We then take

$$V = DE \begin{pmatrix} \lambda_1^{1+s/2} & 0 \\ 0 & \lambda_2^{1+s/2} \end{pmatrix} (DE)^T$$

$$\frac{\partial Q}{\partial t} = (\nabla \cdot V \nabla)(\nabla \cdot \nabla) Q, \qquad (2)$$

The tensor formulation preserves the length scaling used on uniform grids while also accounting for both Δx and Δy length scales which can be different in distorted elements which appear in the mesh transition region.

Advantages of tensor-based hyperviscosity:

1. Scale-aware at every quadrature point
2. Better theoretical and practical CFL estimates
3. Improved robustness with respect to underlying meshes
4. In numerical studies, no oscillations or mesh imprinting present
5. Theoretical convergence rates are confirmed

2. New technique for mesh generation

We compare two mesh-generating packages.

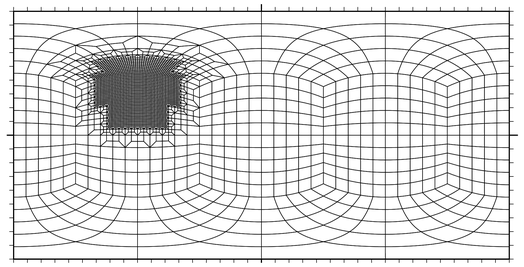

Figure 2: *Different approaches to refined conforming quadrilateral meshes: Highly distorted grid by CUBIT*

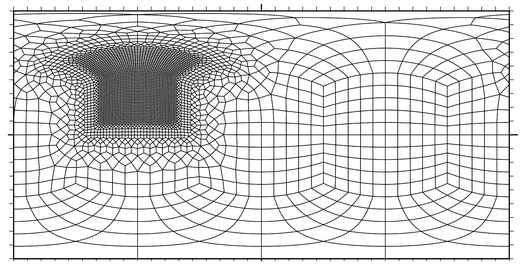

Figure 3: *Different approaches to refined conforming quadrilateral meshes: Low-connectivity grid by SQuadGen*

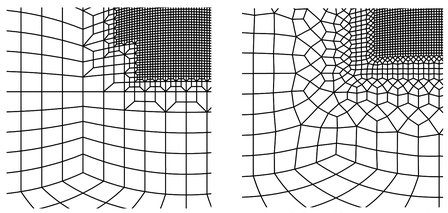

Figure 4: *Nodes with a high valence (left) lead to distorted quadrilaterals. More uniform quadrilaterals with a wider transition region (right).*

For more on SquadGen software, see Paul Ullrich's poster.

Advantages of low-connectivity meshes and SQuadGen:

1. Less distorted elements lead to less expensive computations and to solutions less contaminated with numerical noise
2. SQuadGen produces low-connectivity grids for conforming quadrilateral meshes on a sphere. Capable of developing meshes with only 3-4-5-valence nodes.
3. Flexible smoothing options
4. Input via PNG format

3. Shallow water test cases 2 and 5

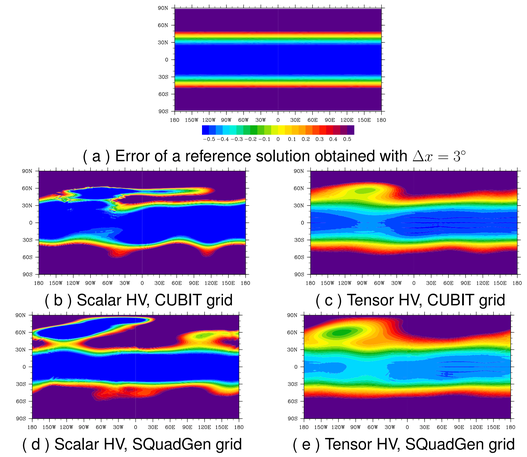

Figure 5: *Error plots for SW test case 2, (b), (c), (d), and (e) have $\Delta x_{coarse} = 3^\circ$ and $\Delta x_{fine} = 0.375^\circ$. In case of scalar HV, plots (b) and (d), the refined region introduces significant numerical noise. While a better quality mesh in (d) improves the outcome, local scales in the refinement are not resolved. Contrary to this, simulations with tensor HV in (c) and (e) are much closer to the uniform solution in (a). In addition, the error in the resolved region is significantly closer to zero.*

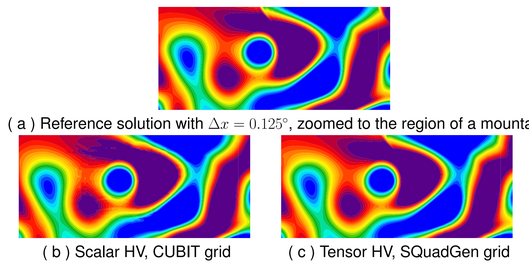

Figure 6: *Vorticity plots for TC5, (b) and (c) have $\Delta x_{coarse} = 3^\circ$ and $\Delta x_{fine} = 0.375^\circ$. Note a prominent numerical noise and mesh imprinting in plot (b) and smooth contours in plot (c).*

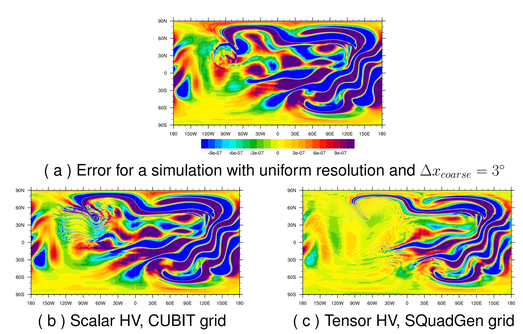

Figure 7: *Error vorticity plots for TC5, (b) and (c) have $\Delta x_{coarse} = 3^\circ$ and $\Delta x_{fine} = 0.375^\circ$. While plot (b) has mesh imprinting and oscillations, plot (c) presents errors near zero for the region within the refinement.*

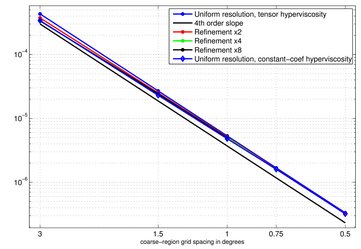

Figure 8: *Measuring effects of local refinement error on global errors for SWTC2 and tensor-based hyperviscosity. We conclude that there is no impact on the global l_2 error. In case of tensor-based hyperviscosity, all four error curves, for the uniform resolution, x2- (scales vary from Δx to $\Delta x/2$), x4- (scales vary from Δx to $\Delta x/4$), and x8- (scales vary from Δx to $\Delta x/8$) refinements, are practically indistinguishable. The errors are controlled by coarse-region scales as they are practically equal to the errors of corresponding uniform resolutions. The convergence rates for studies in this plot are close to 4.0, which coincides with the theoretical rate.*

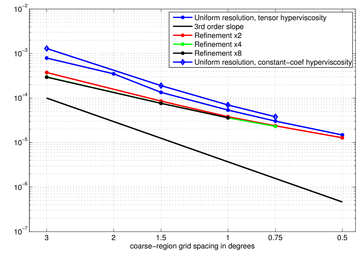

Figure 9: *Measuring effects of local refinement error on global errors for SWTC5 and tensor-based hyperviscosity. Figure confirms that presence of the refinement has no negative impact on global l_2 errors. In fact, the errors are reduced due to the placement of the refined region (over a mountain). The convergence rates slow down as the error approaches the uncertainty in the reference solution.*

4. Conclusions

This work improves CAM-SE's variable-resolution capabilities. Combined settings of meshes with low-valence nodes and tensor-based hyperviscosity as a dissipation prove that
(1) presence of a refined region has no impact on the large scales of the low-resolution region
(2) fine scales in the highly resolved region are fully recovered.

*This research was supported by the Department of Energy Office of Biological and Environmental Research, work package 12-015334 (Multiscale Methods for Accurate, Efficient, and Scale-Aware Models of the Earth System) and work package 11-014996 (Climate Science for a Sustainable Energy Future).